Geophysical and Astrophysical Fluid Dynamics,
Vol. 99, No. 3, June 2005, 199–218

Taylor & Francis
Taylor & Francis Group

Two-dimensional density currents in a confined basin

M. G. WELLS*† and J. S. WETTLAUFER‡

†Department of Geology and Geophysics,
‡Department of Physics, Yale University, New Haven, CT 06520-8109, USA

(*Received 26 September 2004; in final form 1 February 2005*)

We present new experimental results on the mechanisms through which steady two-dimensional density currents lead to the formation of a stratification in a closed basin. A motivation for this work is to test the underlying assumptions in a diffusive "filling box" model that describes the oceanic thermohaline circulation (Hughes, G.O. and Griffiths, R.W., A simple convective model of the global overturning circulation, including effects of entrainment into sinking regions, *Ocean Modeling*, 2005, submitted.). In particular, they hypothesized that a non-uniform upwelling velocity is due to weak along-slope entrainment in density currents associated with a large horizontal entrainment ratio of $E_{eq} \sim 0.1$. We experimentally measure the relationship between the along-slope entrainment ratio, E, of a density current to the horizontal entrainment ratio, E_{eq}, of an equivalent vertical plume. The along-slope entrainment ratios show the same quantitative decrease with slope as observed by Ellison and Turner (Ellison, T.H. and Turner, J.S., Turbulent entrainment in stratified flows, *J. Fluid Mech.*, 1959, **6**, 423–448.), whereas the horizontal entrainment ratio E_{eq} appears to asymptote to a value of $E_{eq} = 0.08$ at low slopes. Using the measured values of E_{eq} we show that two-dimensional density currents drive circulations that are in good agreement with the two-dimensional filling box model of Baines and Turner (Baines, W.D. and Turner, J.S., Turbulent buoyant convection from a source in a confined region, *J. Fluid. Mech.*, 1969, **37**, 51–80.). We find that the vertical velocities of density fronts collapse onto their theoretical prediction that $U = -2^{-2/3} B^{1/3} E_{eq}^{2/3} (H/R)\zeta$, where U is the velocity, H the depth, B the buoyancy flux, R the basin width, E_{eq} the horizontal entrainment ratio and $\zeta = z/H$ the dimensionless depth. The density profiles are well fitted with $\Delta = 2^{-1/3} B^{2/3} E_{eq}^{-2/3} H^{-1} [\ln(\zeta) + \tau]$, where τ is the dimensionless time. Finally, we provide a simple example of a diffusive filling box model, where we show how the density stratification of the deep Caribbean waters (below 1850 m depth) can be described by a balance between a steady two-dimensional entraining density current and vertical diffusion in a triangular basin.

Keywords: Density currents; Entrainment; Upwelling; Stratification

1. Introduction

It has long been recognized that the deepest waters of the world's oceans are formed at high latitudes where surface buoyancy forcing leads to the production of dense cold salty waters, which cascade down the continental slopes as density currents to form deep bottom waters. A similar process can occur in many lakes, whereby differential cooling of the shallow regions drives the production of cold dense fresh waters

*Corresponding author. Email: mathew.wells@yale.edu

Geophysical and Astrophysical Fluid Dynamics
ISSN 0309-1929 print: ISSN 1029-0419 online © 2005 Taylor & Francis Group Ltd
http://www.tandf.co.uk/journals
DOI: 10.1080/03091920500094456

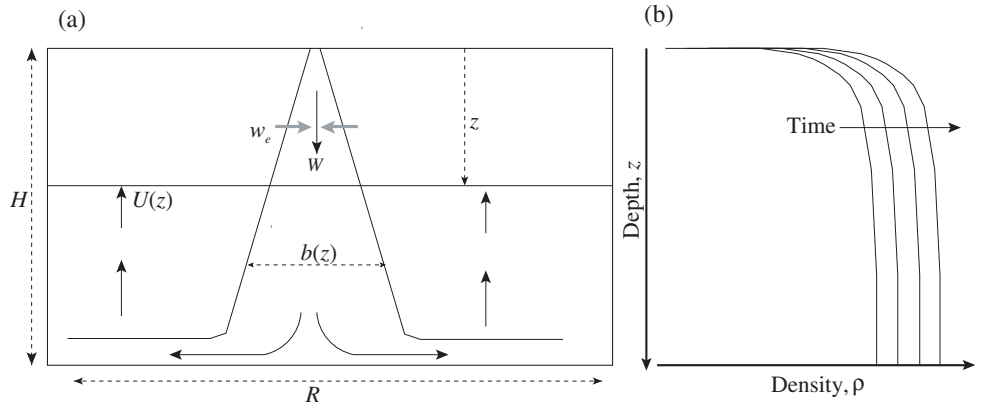

Figure 1. (a) An unstable buoyancy forcing from an isolated source results in an entraining plume or density current. The recirculation of these waters produces a slow upwelling of dense water in the basin with a velocity that decreases as the source of the density current is reached. (b) The re-entrainment of dense waters into the density currents results in the formation of a characteristic density profile that remains constant in shape, while the overall density in the box increases.

that sink and flow down the slopes as entraining density currents. The outflow of these dense waters can then stratify the deeper parts of the basins (Monismith *et al.* 1990, Wells and Sherman 2001, Fer *et al.* 2001, 2002 a,b).

The formation of stratification by a plume in a confined environment was first described in detail in the "filling box" model of Baines and Turner (1969) (hereafter referred to as BT69). Their laboratory plume was made by continuously pumping dense saline water through a small nozzle into the upper surface of a rectangular tank containing water, as shown in figure 1a. This dense water falls under gravity and starts to turbulently entrain the surrounding fluid. The entrainment of the lighter surrounding fluid causes the density within the plume to decrease at the same time as the volume flux increases. Upon reaching the base of the tank the waters spread laterally and a pool of dense water forms. Within the deepening layer of dense water a stratification develops because the density at the base of the plume continues to increase with time due to entrainment of existing waters in the dense pool. It is observed that the entrainment velocity into a free falling negatively buoyant plume is a linear function of the local velocity, and hence the maximum entrainment velocity occurs near the base of the plume. After the pool of dense water fills the depth of the tank, a steady balance between entrainment and upwelling develops, thereby creating the steady density gradient, sketched in figure 1b. The only unknown parameter in the analytic solution of the density gradient (Eq. 9 of BT69) is the entrainment ratio, which is defined by Taylor (1948) as

$$E = w_{\mathrm{e}}/W, \tag{1}$$

where w_{e} is the entrainment velocity normal to the current, which has a mean vertical velocity W. This can be measured independently and has a value $E = 0.1 \pm 0.01$ for free plumes (Morton *et al.* 1956, Turner 1986). Using this empirically determined value, the predicted filling box stratification agrees well with measurements from

a point source plume. Predictions were also made for a line source by BT69 and will be verified in this article.

With a time-varying buoyancy flux driving the turbulent plume, Killworth and Turner (1982) found that the plume only reaches the base of the tank during times of peak buoyancy forcing, and otherwise spreads at intermediate depths when reaching its level of neutral buoyancy. The resulting stratification is almost identical to that created by a constant plume with the maximum value of the buoyancy forcing. When multiple plumes of different strengths are used, the overall stratification was the same as that resulting from the strongest plume, with the outflow from the weaker plumes intruding at their level of neutral buoyancy (Wong and Griffiths 1999). When adding weak rotation to the filling box problem, Pierce and Rhines (1996) also found the same density profiles as in the non-rotating case. Due to the robust nature of the filling box theory, it has been used to explain the formation of stratification by diverse arrangements of buoyancy sources in a variety of geophysical and engineering contexts (e.g. Turner 1986, Linden 1999).

The same filling box process can occur in a basin where strong convection over shallow shelf regions leads to periodic formation of a dense line plume that stratifies the deep basin, as shown in figures 2 and 3. Because a density current only entrains on one surface, rather than two for a two-dimensional plume, it can be considered to be one-half of the plume shown in figure 1. Ellison and Turner (1959), (hereafter referred to as ET59) conducted seminal work on how the along-slope entrainment rate E in density currents varied as a function of slope and Richardson number, and found that E decreases with slope. The formation of stratification in the deep basin from convection on a shelf slope was investigated experimentally by Turner (1998); using a steep 45° slope he observed the development of circulation patterns very similar to the filling box model. Detailed field observations have been made in small inland lakes (Fer *et al.* 2001, 2002a,b, Wells and Sherman 2001) and show that during sustained periods of winter cooling, significant stratification can be formed in a manner that is qualitatively similar to the filling box model. For deep-water formation the forcing need not be localized in space above the shelf because a spatially uniform cooling will result in more rapid cooling of the shallow regions of the lake. If these shallow regions occupy a significant fraction of the lake, then the resulting density currents will stratify the remaining deep regions and form a slowly upwelling thermocline.

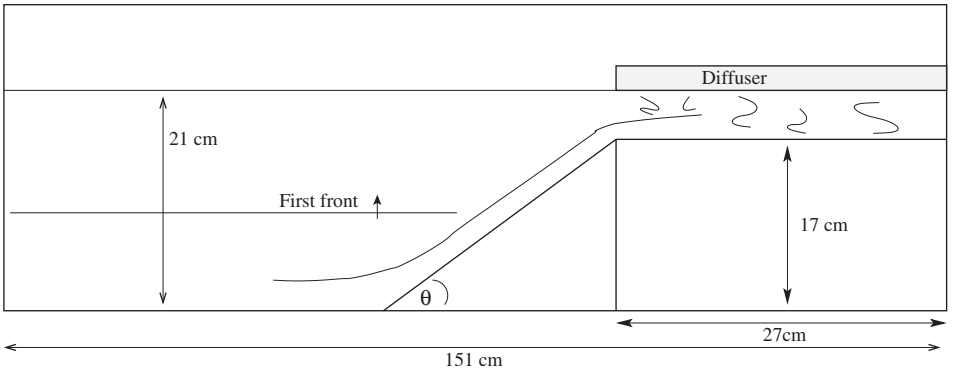

Figure 2. An illustration of the experimental setup. Slope angles of 16, 27, 45, 60, 75 and 89° were used.

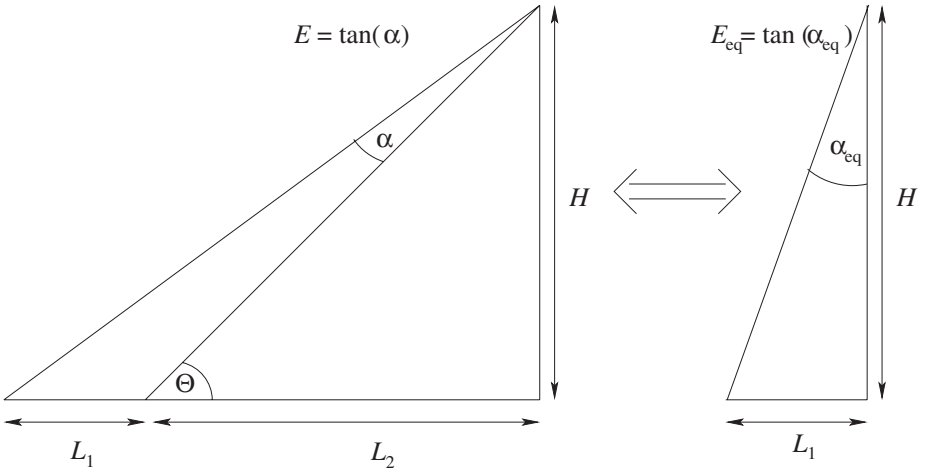

Figure 3. The entrainment ratio is the ratio of entrainment velocity to along-slope velocity, $E = w_e/W$ (ET59), and is related to the rate at which the plume increases horizontal width as a function of depth $E_{eq} = db/dz$ (BT69) by using the relation derived by HG05 that $E_{eq} = E/\sin(\Theta)$. This can be simply visualized in the figure above. On the left the entrainment rate E is related to the angle α, by $E = \tan(\alpha)$. On the right we have an equivalent plume that increases the same horizontal width L_1 in a depth H but has $\alpha_{eq} > \alpha$, implying a larger equivalent horizontal entrainment.

This non-uniform upwelling can balance the downwards mixed-layer growth, thereby creating a steady mixed-layer depth as the lake continues to cool (Wells *et al.* 1999, Wells and Sherman 2001).

In an oceanographic setting, the vertical upwelling of dense water can be balanced by effective downwards small scale mixing of lighter surface waters, so that a constant density profile emerges. This can be represented by a diffusive "filling box", first introduced by Manins (1973, 1979) to describe the density stratification of the deep Red Sea. A similar but more complex model was developed by Hughes *et al.* (2005), and Hughes and Griffiths (2005) (referred to as HG05 hereafter) whereby the world's oceans are represented by a single basin with the deep water being formed at high latitudes. A critical assumption in their theory is that the entrainment by the density current will result in vertically non-uniform upwelling within the basin, similar to the filling box dynamics. The entrainment velocity normal to the bottom slope in such oceanographic density currents is generally very small, but they showed that it is actually the rate of increase of volume flux with depth rather than the along-slope rate of increase that is the important quantity. The two are related by $E_{eq} = E/\sin(\Theta)$ where Θ is the angle measured relative to the horizontal at which the plume descends a slope. By extrapolation of the ET59 data they predicted that $E_{eq} = 0.1$ at small slopes. This implies that upwelling velocities in the world's oceans are vertically non-uniform, as in the filling box model. A balance between uniform upwelling and downwards vertical diffusion was shown by Munk (1966) to result in a realistic shape of the density distribution, if the vertical eddy diffusivity, κ, has a value of $10^{-4}\,m^2\,s^{-1}$. Field observations have found that a more realistic value of κ is an order of magnitude lower (Gregg 1989, Ledwell *et al.* 1993, Toole *et al.* 1994), leading many to assume that the Munk (1966) model was incorrect. However, HG05 showed that the density distribution produced by a non-uniform upwelling balanced

by downwards diffusion, with observed meridional heat flux as a boundary condition, is similar to realistic basin-averaged ocean stratifications, and has a realistic eddy diffusivity that is an order of magnitude lower than that of Munk (1966).

This article is organized in the following way. We start in the following section by revisiting the work of BT69, who made detailed predictions of the form of the stratification created by a vertical two-dimensional plume. These observations have not been previously tested in the laboratory and in section 3 we detail a series of experiments that demonstrate how this theory also describes a filling box driven by a turbulent density current on a slope, in addition to the vertical two-dimensional plume originally considered. We also experimentally verify the crucial connection between the horizontal entrainment ratio of the density current and the entrainment normal to the density current. In section 4, we discuss the predictions of HG05 in light of our experimental observations, and show how the observed density profile of the deep Caribbean basin can be described by a similar balance between non-uniform upwelling and vertical diffusion.

2. Theory

In order to make this presentation reasonably self contained, and to develop the scaling of particular relevance to our experiments, we revisit the theory of BT69. The conservation equations for volume, momentum and density deficiency in a two-dimensional line plume, when integrated over the cross section of width b are

$$\frac{\mathrm{d}}{\mathrm{d}z}(bw) = 2Ew, \tag{2}$$

$$\frac{\mathrm{d}}{\mathrm{d}z}(bw^2) = b\Delta, \tag{3}$$

$$\frac{\mathrm{d}}{\mathrm{d}z}(bw\Delta) = bw\frac{\partial \Delta_\mathrm{o}}{\partial z}, \tag{4}$$

where E is the entrainment ratio, w is the vertical plume velocity, the gravity anomaly of the plume is $\Delta = g(\rho - \rho_1)/\rho_1$ and the gravity anomaly of the environment is $\Delta_\mathrm{o} = g(\rho_\mathrm{o} - \rho_1)/\rho_1$, in which g is the gravitational acceleration, ρ and ρ_o are the densities inside and outside the plume and ρ_1 is a reference density.

For the present experiment, density changes in the environment at any level occur only because of vertical motion, so that

$$\frac{\mathrm{d}\Delta_\mathrm{o}}{\mathrm{d}t} = -U(z)\frac{\mathrm{d}\Delta_\mathrm{o}}{\mathrm{d}z}. \tag{5}$$

In section 4.1, we will discuss the influence of vertical mixing or diffusion. The upward volume flux in the environment must equal the downward flux in the plume, which gives

$$-RU = bw, \tag{6}$$

where U is the upwelling velocity of the environment and R is the basin width. An important assumption in the BT69 model is that the basin width is much larger than the horizontal width of the density current, so that $R \gg b$. This can be easily satisfied in the laboratory, and in most oceanographic applications where the horizontal cross-sectional area of the density current is much less than that of the basin. The implications of having $R \sim b$ have been considered by Barnett (1991), who found very different circulations driven by momentum.

Generalization of the results of BT69 from a vertical two-dimensional plume to the case of a two-dimensional density current on a slope, requires that the horizontal entrainment ratio E_{eq} be determined. In the ET59 model, the entrainment ratio is defined in terms of the rate of increase in plume width as a function of the distance along slope, whereas BT69 define the entrainment ratio as the rate of increase in horizontal plume width as a function of depth, which we denote as E_{eq}. For a density current flowing vertically the two definitions are the same, but for a density current on a slope they can be quite different. HG05 showed that by making the simple co-ordinate transformation from along-slope position to vertical depth, the two definitions are simply related by

$$E_{\mathrm{eq}} = E/\sin\Theta, \tag{7}$$

where Θ is the slope angle. For a vertical plume the entrainment velocity is already horizontal so the two definitions are the same, but when the slope decreases, E_{eq} diverges from E. This is illustrated in figure 3. The measured entrainment values of ET59 are consistent with $E \to 0$ as the slope goes to zero, and HG05 assumed a linear interpolation between the measured value at laboratory slopes ($E = 10^{-2}$ at $\Theta = 5^{\circ}$) and the theoretical limit that $E \to 0$ as $\Theta \to 0$. They concluded that at low slope angles E_{eq} would asymptote to 0.1. Tests of this assumption will be described herein.

The equations (2)–(5) are non-dimensionalized by

$$\Delta_{\mathrm{o}} = 2^{-1/3} B_{\mathrm{o}}^{2/3} E_{\mathrm{eq}}^{-2/3} H^{-1} \Delta_{\mathrm{o}}(\zeta, \tau), \tag{8}$$

$$\Delta = 2^{1/6} B^{2/3} E_{\mathrm{eq}}^{-2/3} H^{-1} \Delta(\zeta), \tag{9}$$

$$w = 2^{1/3} B^{1/3} E_{\mathrm{eq}}^{-1/3} w(\zeta), \tag{10}$$

$$b = E_{\mathrm{eq}} H b(\zeta), \tag{11}$$

$$U = 2^{-2/3} B^{1/3} E_{\mathrm{eq}}^{2/3} (H/R) U(\zeta), \tag{12}$$

$$t = 2^{2/3} B^{-1/3} E_{\mathrm{eq}}^{-2/3} R\tau \quad \text{and} \tag{13}$$

$$\zeta = z/H. \tag{14}$$

The above non-dimensionalization will hold for a filling box produced by a density current, except that the density current only entrains on one side, the basin scale R

is half of that used in figure 1. The resulting dimensionless versions of differential equations (2)–(4) and (6), are

$$\frac{\mathrm{d}U}{\mathrm{d}\zeta} = -w, \qquad \frac{\mathrm{d}(wU)}{\mathrm{d}\zeta} = -\Delta b, \tag{15, 16}$$

$$\frac{\mathrm{d}(U\Delta)}{\mathrm{d}\zeta} = U\frac{\mathrm{d}\Delta_\mathrm{o}}{\mathrm{d}\zeta}, \qquad U\frac{\mathrm{d}\Delta_\mathrm{o}}{\mathrm{d}\zeta} = 1. \tag{17, 18}$$

Solutions can be found for all these variables, but for the present discussion the important results are in the form of the upwelling velocity U and the environmental density Δ_o. The mean velocity of a two-dimensional steady turbulent density current has been observed to be constant in ET59; hence $w(\zeta) = 1$. From (15) such a constant velocity implies that the width grows linearly with depth and $b = \zeta$. A dimensionless version of the equation of continuity (6) is that $U = -bw$, so this leads to an upwelling velocity that is also a linear function of depth, $U = -\zeta$. Such an upwelling velocity implies that the position ζ of density fronts will vary with time as

$$\zeta = \exp(-\tau). \tag{19}$$

A linear upwelling velocity combined with (18) implies that the environmental density has a profile like

$$\Delta_\mathrm{o} = \ln(\zeta) + \tau, \tag{20}$$

where the constant is evaluated using the fact that the total buoyancy in the tank increases at a rate determined by buoyancy flux normalized by tank volume. At the base of the tank the density Δ_o has a maximum, and the density gradients $\mathrm{d}\Delta_\mathrm{o}/\mathrm{d}\zeta$ are a minimum. Near the surface, where $\zeta \to 0$, there is a minimum in Δ_o and a maximum in $\mathrm{d}\Delta_\mathrm{o}/\mathrm{d}\zeta$; similar to the sharp pycnocline in the ocean.

The origin of the maximum in the buoyancy gradient $\mathrm{d}\Delta_\mathrm{o}/\mathrm{d}\zeta$ as $\zeta \to 0$ is due to the intimate connection between the density gradients and the local upwelling velocity as described by equation (5). The rate of change of buoyancy is just the buoyancy flux per unit length divided by the cross-sectional area A; $\mathrm{d}\Delta_\mathrm{o}/\mathrm{d}t = B/A$. Hence in (5) there is an inverse relationship between the upwelling velocity and density gradient, with the maximum density gradients occurring at the surface due to the weak entrainment velocities of the narrow plume. In our laboratory experiments molecular diffusion is not important for the typical length and time scales, however as we will discuss in section 4, for oceanographic applications a much larger "eddy diffusivity" is important in the vertical density balance.

Thus far we have only considered the case where the basin has a constant width with depth. However, it is easy to include a new dimensionless variable $R(\zeta)$ in the continuity equation (6). A good approximation to the geometry of many realistic ocean or lake basins is that of a triangular wedge (rather than a constant width rectangular basin) so that $R(\zeta) = (1 - \zeta)$. If $w = 1$ the variation in width creates only a change to the upwelling velocities at depth, with $U = -\zeta/(1 - \zeta)$. Due to the relation between density gradients and vertical velocity expressed by (5), these faster upwelling velocities

at depth then imply that there will be weaker density gradients here. Because the density gradients are already weak at this depth, in practice this is only a small correction.

3. Experiment

The experiments on two-dimensional density currents were performed in the tank illustrated in figure 2. The tank has a length of 150 cm, a width of 12 cm and a depth of 25 cm. A horizontal shelf of length 20 cm and height 17 cm was created, onto which dense saline water was pumped through a diffusing manifold that sat 2 cm above the shelf. This dense saline water created a horizontal exchange flow, with the dense saline water flowing down the slope. During the descent of this dense water down the slope, entrainment of ambient fluid decreases its density and hence increases its volume. The resulting movements of the dyed density layers were recorded with digital photographs, as shown in figure 4. Seven experiments were performed at slopes Θ ranging between 16 and 90°. Fluid of density $\rho = 1.05\,\mathrm{g\,cm^{-3}}$ was pumped at flow rates of $Q = 1.5\,\mathrm{cm^3 s^{-1}}$, resulting in buoyancy fluxes per unit width of $B = gQ(\rho - \rho_o)/\rho_o W = 5.8\,\mathrm{cm^3\,s^{-3}}$. The density currents have Reynolds number of the order 300–500. Two experiments (not reported here) were conducted with 45° slopes in a larger tank at $\mathrm{Re} = 1000$ and essentially the same results were found for entrainment rates and velocity profiles, indicating a lack of Reynolds number dependence for these flows.

3.1. *Experimental results*

We present two sets of experimental results – firstly, velocity and density measurements that confirm the theoretical scalings of BT69, and secondly, measurements of the equivalent entrainment ratio E_{eq}, which is predicted by HG05 to asymptote to a constant value at low slope angles.

In figure 5a we show a photograph of a green density current flowing down a 60° slope into a tank 13 min after the initiation of the experiment. Layers of red and yellow dye from earlier density currents can be seen. The vertical blue lines in this image mark the position and extent from which thin vertical slices are taken every 10 s. These slices are stacked and show the complete time history of the positions of the various waters from the dyed density currents in figure 5b. On top of this time history we have overlain the theoretical prediction that $\zeta = \exp(-\tau)$. There is good agreement with the theory, except, as expected, at the very bottom and top. At the base, the finite thickness of the outflowing density current gives the appearance of very large vertical velocities. At the surface of the tank, the velocities do not vanish due to the small amount of saline fluid that is continually being pumped through the manifold on the shelf, whereas the theory of BT69 assumed an idealized source of buoyancy that had no volume flux.

Figures 5b and c clearly show the inverse relationship between velocity and density gradient expressed by equation (5), with maximum velocities occurring where the density gradients are the weakest. In figure 5b the movement of density fronts follows $\zeta = \exp(-\tau)$ so that $U = -\zeta$, while in figure 5c we find that the experimental measurements of the density profile have $\Delta_o = \ln(\zeta) + \tau$ so that $\mathrm{d}\Delta_o/\mathrm{d}\zeta = 1/\zeta$; hence $U\,\mathrm{d}\Delta_o/\mathrm{d}\zeta = -1$ as required by (5).

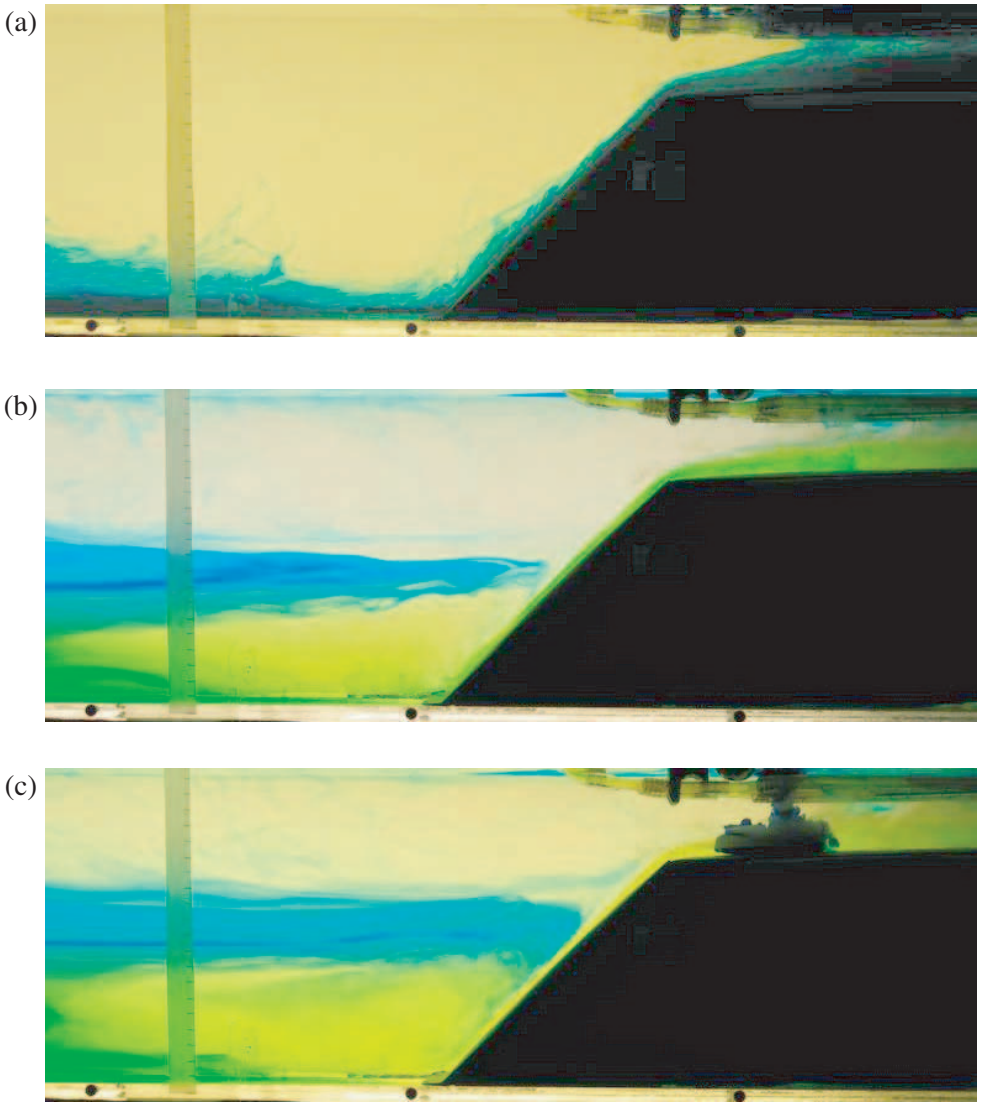

Figure 4. Photographs of a density current on a 45° slope with $B = 5.8\,\mathrm{cm^3\,s^{-3}}$, showing the vertical movement of dyed density layers at times (a) $t = 0$, (b) $t = 320\,\mathrm{s}$, (c) $t = 400\,\mathrm{s}$.

In figure 6 we plot the vertical position of density fronts *versus* time for a series of experiments with varying slope, but constant buoyancy forcing. Once allowance is made for the variation of the entrainment ratio with slope, then all the measured data collapse onto the predicted curve. The entrainment ratio, E_{eq}, is the only free parameter, and is deduced by fitting the theoretical curve to the data. These measured values of E_{eq} and inferred values of E [using (7)] are plotted in figure 7, along with the original measurements of entrainment in density currents from ET59. The error bars in our data are mainly due to the unavoidable presence of internal waves in the filling box process (Wong *et al.* 2001). There is very good agreement between the present inferred values of E and the ET59 results in figure 7b, where the entrainment vanishes as slope

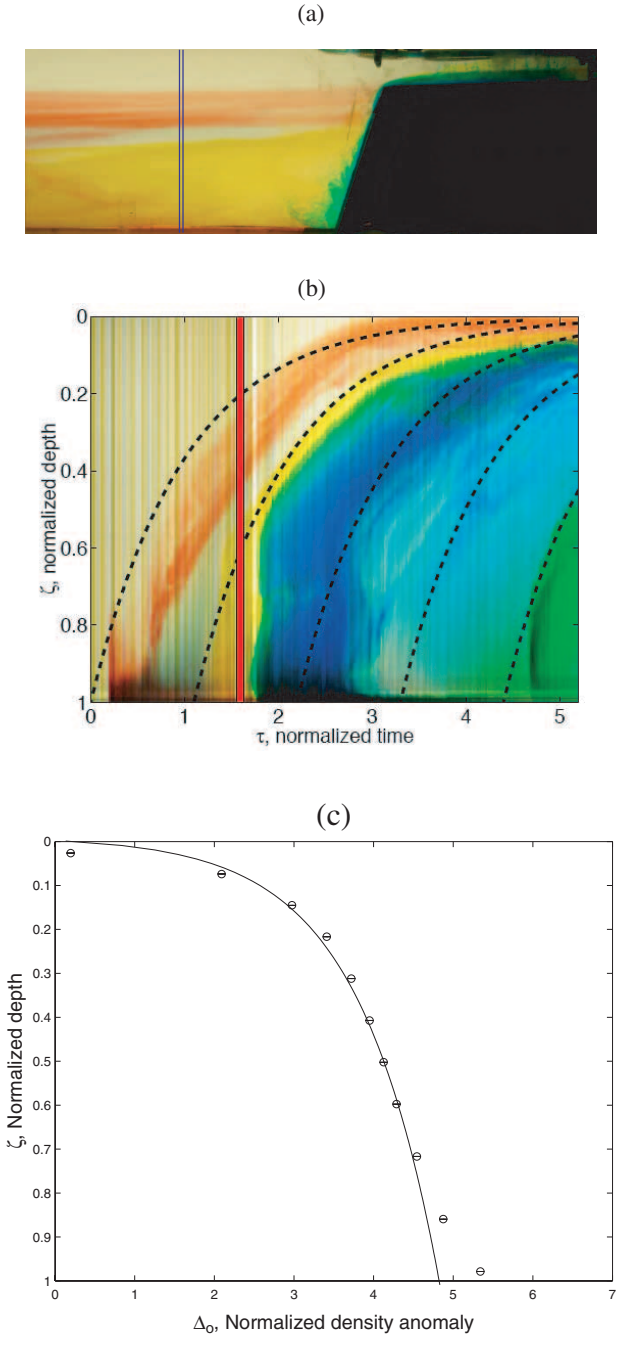

Figure 5. (a) Experimental observations of a density current at time $\tau = 1.53$. The two blue vertical lines mark the sections that are stacked in the depth *versus* time plot of (b). The vertical movement of the density fronts can be clearly seen, and agrees well with the theoretical prediction that $\tau = \ln(1/\zeta)$. The vertical red line marks the temporal position of the photograph in (a). The dimensionless density profile is plotted against the theory that $\Delta_o = \ln(\zeta) + \tau$ in (c). Samples were taken from the same experiment as (b) at $\tau = 4.8$, and the density was determined by measuring the conductivity of the saline samples. In this experiment the buoyancy flux was $B = 6.125\,\mathrm{cm^3 s^{-3}}$ and we assume $E_{eq} = 0.08$ in fitting the theoretical curves.

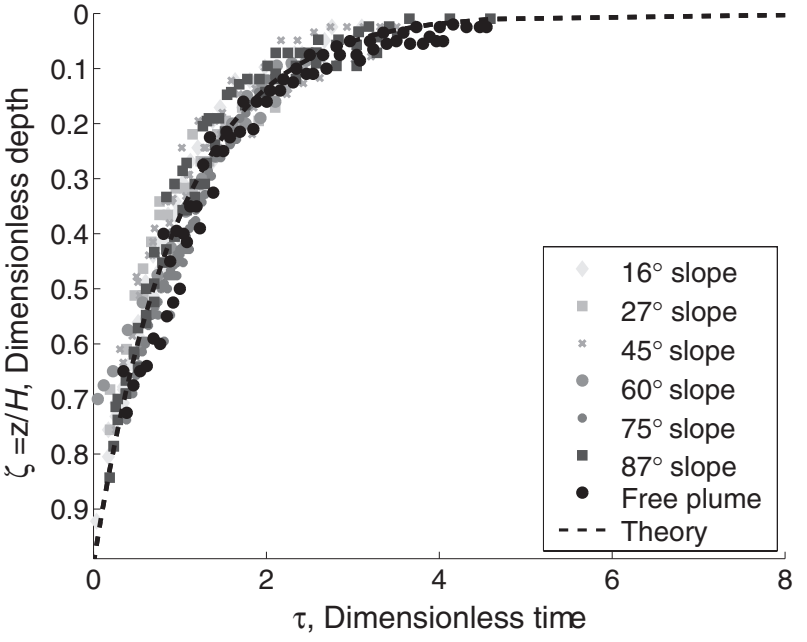

Figure 6. The experimental observations of the vertical position of density fronts *versus* time are plotted against the theoretical prediction, for a series of six experiments similar to those shown in figures 4 and 5 where $16^\circ < \Theta < 90^\circ$ and one experiment with a free plume. Once allowance is made for the dependence of entrainment ratio E_{eq} with slope, there is good agreement with the theoretical prediction. In these experiments $B = 5.8\,\mathrm{cm^3\,s^{-3}}$.

angle $\Theta \to 0$. However, the entrainment ratios that are appropriate for use in a filling box model appear to asymptote to a constant value of approximately $E = 0.08$ as $\Theta \to 0$, similar to the prediction of HG05. Neither our present experiments nor ET59 give a sense of exactly what the functional form of E or E_{eq} is for $\Theta < 10^\circ$, and the functional form of E_{eq} deduced from (7) is very sensitive to how E approaches zero. It must decrease more rapidly than linearly if E_{eq} is to maintain realistic values. As we will describe in the next section, this limit is important because most oceanographic density currents exist on slopes with $\Theta < 10^\circ$.

The fact that the position of the first front is well described by $\zeta = \exp(-\tau)$ for all the experiments for 16–90° slopes implies that the entrainment is occurring over the full length of all the density currents. If the gravity currents were laminar then the upwelling velocity would be constant below the level of the sill, that is, like $\zeta \propto -\tau$. This is clearly not seen in the data of either figure 5(b) or 6. A laminar density current would also result in a uniform density in the basin, rather than the observed profile in figure 5(c). This upwelling implied by the entraining density current had been implicitly assumed in the successful interpretation of field observations of Wells and Sherman (2001), where bottom slopes had $\Theta < 10^\circ$. The fact that weakly entraining density currents can still force a strongly non-uniform upwelling is also the essential difference between Munk's (1966) theory of oceanic stratification and that of HG05, discussed in the next section.

Another important oceanographic implication of the constant equivalent entrainment rate of density currents shown in figure 7a is that the initial depth at which

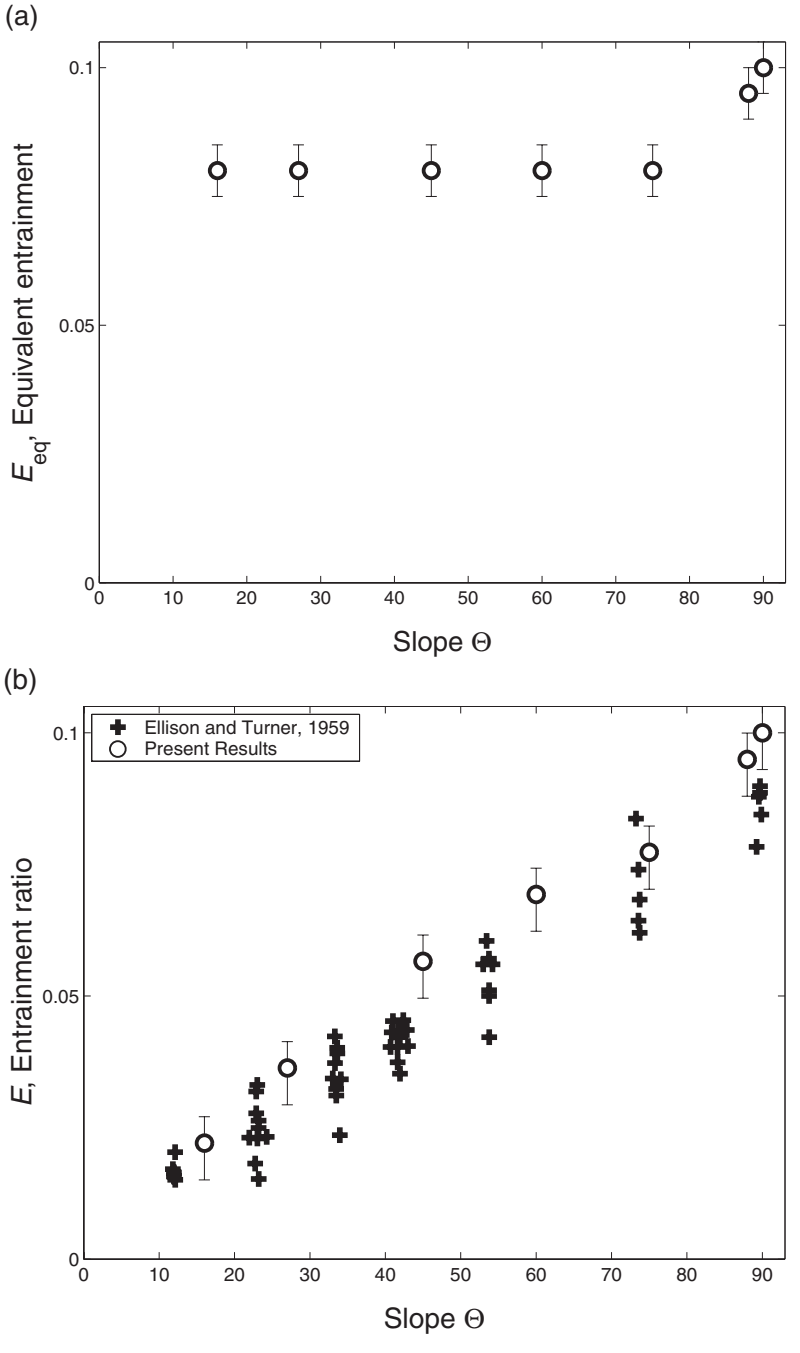

Figure 7. In fitting the theoretical profile (19) to the laboratory data of figure 6 we determine the equivalent entrainment ratio E_{eq} of the density currents on slopes, which is plotted in (a). The free plume and density current on the 87° slope both have a value of $E_{eq} \approx 0.1$, as expected, but at lower slopes E_{eq} appears to asymptote to a value of $E_{eq} = 0.08 \pm 0.005$. This confirms the prediction of HG05 that density currents on low angle slopes should entrain fluid horizontally at rates comparable to an equivalent vertical plume. In (b) we plot the estimated along-slope entrainment rate E (plotted as circles) using equation (7), and we find good quantitative agreement with the previous experiments of ET59, (+).

a density current intrudes into a linear stratification should be independent of the slope and depend only upon the background stratification and the buoyancy flux of the density current. This has been found in initial experiments for density currents in stratified environments on 45 and 90° slopes (Wells and Wettlaufer 2005), where the depth of intrusion is observed to be the same for both the cases, when the same buoyancy flux and stratification was used. The scaling observed of $Z \propto B^{1/3}/N$ is the same as in the previous experiments of Wright and Wallace (1979) and Bush and Woods (1999) for free two-dimensional plumes. The along-slope entrainment rate for a 45° slope is less than that for a 90° slope, and hence one might have naively expected that intrusion depth of density currents on 45° slopes would be systematically deeper. Currently we are testing if such scaling holds for shallower slopes.

4. Oceanographic application

Most observations of oceanographic entrainment (see, for example, Baringer and Price 1999) choose to describe the entrainment ratio as a function of local Froude number rather than the slope angle. The experimental data of ET59 can be well described by $E \sim 0.08\mathrm{Fr}$, where the Froude number is defined as

$$\mathrm{Fr} = \frac{W}{\sqrt{g'h\cos\Theta}}, \tag{21}$$

which reduces to the more common definition of $\mathrm{Fr} = W/\sqrt{g'h}$ as $\Theta \to 0$.

In figure 8 we plot a range of observations of entraining density currents from the laboratory (ET59, Alavian 1986, Cenedese *et al.* 2004) and the field (Baringer and Price 1999, Dallimore *et al.* 2001, Princevac *et al.* 2004). It has been suggested (Jim Price, personal communication, 2004) that the data at low Froude number ($\mathrm{Fr} < 1$) can be fitted by $E \propto \mathrm{Fr}^8$ and the data at high Froude number ($\mathrm{Fr} > 1$) by $E \propto \mathrm{Fr}$. The values of entrainment ratio E for $\mathrm{Fr} < 1$ are very small but non-zero. Most of the previous interpretations of the ET59 data (i.e., Turner 1986; or Price and Baringer 1994) had assumed that there was a cut-off Froude number around $\mathrm{Fr} = 1$ below which no entrainment occurred in density currents, and this assumption has since been used in a large number of modeling studies. Using equation (7) HG05 extrapolated the data of ET59 to small slope angles and predicted that $E_{\mathrm{eq}} = 0.1$, similar to our laboratory observations. Thus, rather than there being a cut-off at low slopes or low Froude numbers, density currents are still able to modify the environment via a filling box process. Most of the observations in oceanic settings shown in figure 8 have found $\mathrm{Fr} \sim 1$ and $E = 10^{-4}$ to 3×10^{-3} for $\Theta = 0.1$ to 1°, much lower than the smallest value of entrainment in our experiments or ET59, where $E = 0.015$ when $\Theta = 9°$. Using equation (7) shows that for a low slope of $\tan\Theta = 1/25$ with $E = 10^{-4}$, values of $E_{\mathrm{eq}} = 0.1$ are possible, but due to the large scatter in the data of field experiments, E_{eq} values between 0.05 and 0.3 are also possible. The important point, however, is that it is very reasonable to expect that a density current flowing down a low angle slope in a confined basin will be able to modify the stratification via a filling box process, and that the density current will be able to force a vertically non-uniform upwelling. An example of such a filling box process can be found in the

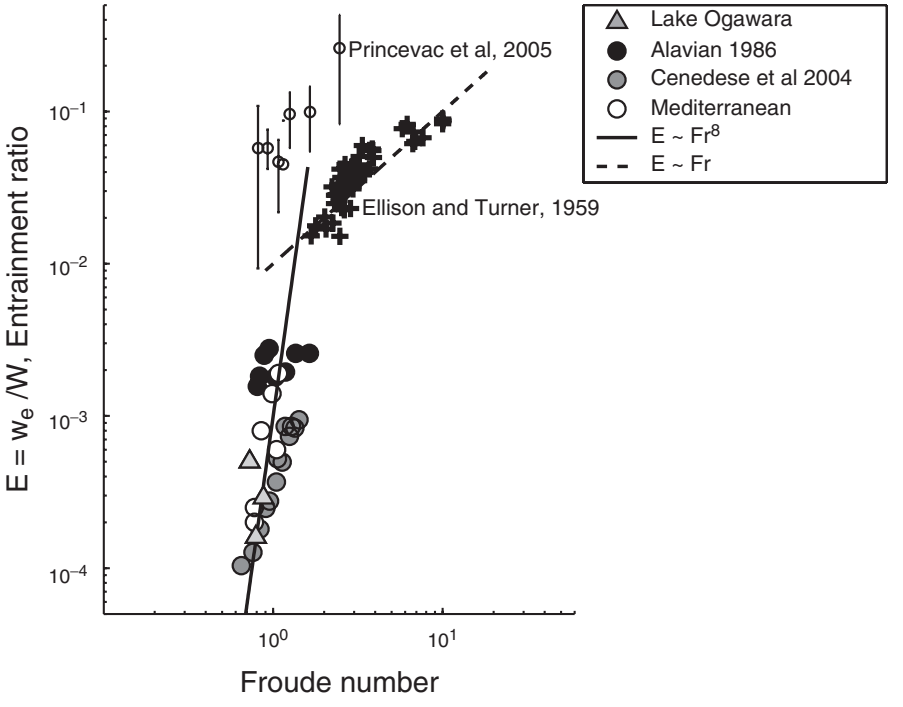

Figure 8. Entrainment ratio $E = w_e/W$ as a function of Froude number. Data from laboratory experiments of ET59, Alavian (1986) and Cenedese *et al.* (2004) are shown, as well as field observations in the Mediterranean (Baringer and Price 1999), Lake Ogawarra (Dallimore *et al.* 2001) and recent field observations of a katabatic flow at high Froude number and Reynolds number of 10^7 (Princevac *et al.* 2005).

field observations of dense water formation in winter in the shallow water of the Chaffey Reservoir (Wells and Sherman 2001). The presence of persistent stratification over two winters (rather than the typical winter overturning of the water column) was attributed to a non-uniform upwelling driven by density currents from the shallow regions, balancing downwards penetrative convection from surface cooling, resulting in a fixed mixed-layer depth as the whole water column continued to cool.

4.1. *Diffusive–advective balance*

If a steady state is to be achieved by the continued supply of dense waters at the floor of an oceanic basin, then there must be a balance between the advection and diffusion in the vertical. This was first discussed by Munk (1966) in terms of high-latitude waters providing the deep bottom waters of the world's oceans. These cold dense waters were assumed to rise slowly with a uniform velocity U, which was balanced by mixing of lighter surface waters downwards to achieve a steady density profile. Munk (1966) then showed that one can solve the diffusion–advection equation

$$U\frac{\partial \Delta}{\partial z} = \kappa \frac{\partial^2 \Delta}{\partial z^2} \tag{22}$$

with an exponential solution of the form

$$\Delta = \Delta_{z=0} \exp(-zU/\kappa). \tag{23}$$

This was originally proposed to explain the shape of the stratification in the world's oceans. Estimated rates of high-latitude bottom water production, Q can be converted into an estimate of U by assuming uniform vertical upwelling everywhere, producing $U \sim 10^{-7}\,\mathrm{m\,s^{-1}}$ for the global mean, with $\kappa \sim 10^{-4}\,\mathrm{m^2\,s^{-1}}$. This estimate of κ has since been found to be an order of magnitude too high compared with the field observations (Gregg 1989, Ledwell *et al.* 1993, Toole *et al.* 1994).

A solution to this problem was proposed by HG05, wherein entrainment (albeit small) into sinking currents is assumed and hence a non-uniform upwelling is predicted. If the dense waters descend to the abyssal ocean as entraining density currents, then the upwelling vertical velocity U will be a function of depth, with a maximum upwelling velocity at the outflow level of the density current. For the simplest case of a two-dimensional plume in our laboratory experiment the vertical velocity has the form $U(z) = U_\mathrm{o}\,(z/H)$, and a balance between vertical advection and diffusion results in an error-function solution for the density profile

$$\Delta = \Delta_{z=0} \operatorname{erf}\left(-z\sqrt{U_o/H\kappa}\right) \tag{24}$$

As shown in figure 9 both equations (23) and (24) have a similarly shaped solution for the density. The important difference between the two expressions is the H in the exponent of (24). For deep basins where H is of the order of kilometers, the implication is that the value of the eddy diffusivity κ can be smaller for the same magnitude of vertical upwelling velocity U. HG05 considered a similar but more realistic treatment of an oceanic density current formed at high latitudes that includes bottom drag and the Coriolis forces, and concluded that this simple difference in the form of the upwelling velocities may explain the difference between the large value of $\kappa = 10^{-4}\,\mathrm{m^2\,s^{-1}}$ required by Munk (1966), and the lower observed values of $\kappa = 10^{-5}\,\mathrm{m^2\,s^{-1}}$ (Gregg 1989, Ledwell *et al.* 1993, Toole *et al.* 1994) that are typically observed in the world's oceans. By applying the observed meridional heat transport as a boundary condition, they also predict the top-to-bottom density difference and overturning flux for the global ocean, and hence also the scale U_o.

4.2. *Stratification of the deep Caribbean basin*

As a practical example of equation (24), let us consider the stratification of the deep Caribbean basin, which has been observed by MacCready *et al.* (1999) to be periodically ventilated below a depth of 1850 m by a dense cold density current that episodically flows through the Jungfern–Grappler sill complex. The observed current had an initial width of about 5–10 km and a depth of up to 200 m. Upon entering the Jungfern–Grapeler sill complex, the density current turns to the right under the influence of the Coriolis force and then descends slopes between 1/4 and 1/100. At 5, 13 and 22 km downstream the plume was observed by MacCready *et al.* (1999) to have a width of between 10 and 15 km and was spread along the slope over a range of 1000 m depth. At about 50 km downstream, the plume started to detrain at

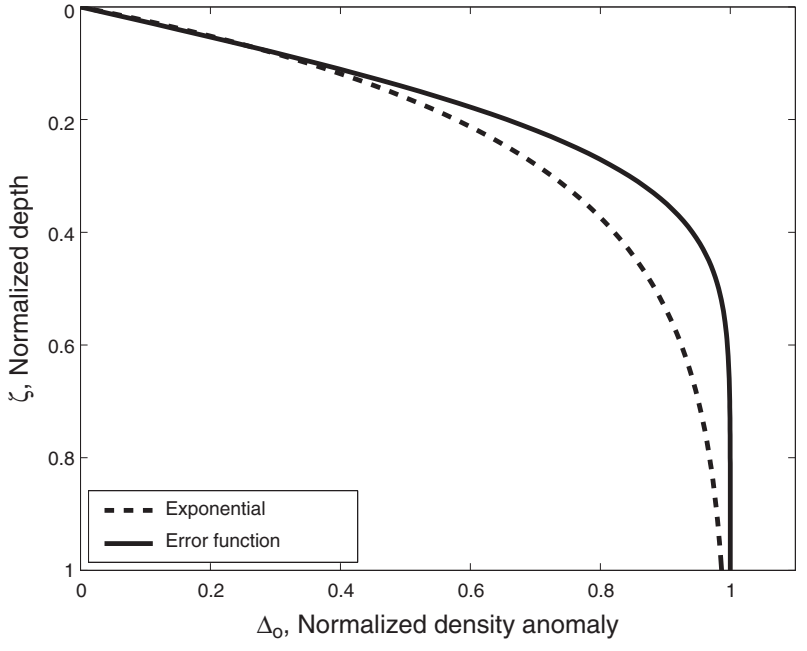

Figure 9. A comparison of equations (23) and (24) for the same values of $U_o = 1.4 \times 10^{-4}\,\mathrm{m\,s^{-1}}$, with $\kappa_{\mathrm{exp}} = 1.3 \times 10^{-4}\,\mathrm{m^2\,s^{-1}}$ $\kappa_{\mathrm{erf}} = 5 \times 10^{-5}\,\mathrm{m^2\,s^{-1}}$, and $H = 4\,\mathrm{km}$. This shows the essential idea of HG05, that with the same value of mean upwelling velocity U a similar vertical density gradient results from (24) with about half the vertical eddy diffusivity used in (23).

a level between 300 and 800 m beneath the sill. We will implicitly assume that the density current is steady in the following, even though MacCready *et al.* (1999) noted that the density current was episodic with ~10 events occurring per year. We argue that the steady-state assumption is reasonable, in light of the time-periodic filling box experiments of Killworth and Turner (1982). They found that even though the plume would only reach the base of the tank in a fraction of the time, the resulting stratification was virtually the same as that for a steady plume. Furthermore, because the stratification is inversely proportional to the average vertical velocity, it is also reasonable to assume that the average upwelling velocity is the same as that of a steady density current or plume. We will also assume that the increase in cross-sectional area with the depth of the density current is approximately linear, so that we can use a two-dimensional representation of the density current and hence apply (24) to describe the steady stratification in the basin.

The depth distribution shown in figure 10 closely resembles a simple wedge, so that the basin length can be considered to vary as $R(\zeta) = R_{\mathrm{o}}(1 - \zeta)$. By considering the continuity of fluid, equation (6), within such a basin, a descending entraining density current with a constant velocity would create a vertical velocity U of the form

$$U(\zeta) = U_{\mathrm{o}} \frac{\zeta}{1 - \zeta}, \tag{25}$$

where $U_{\mathrm{o}} = E w_{\mathrm{o}} H / R_{\mathrm{o}}$.

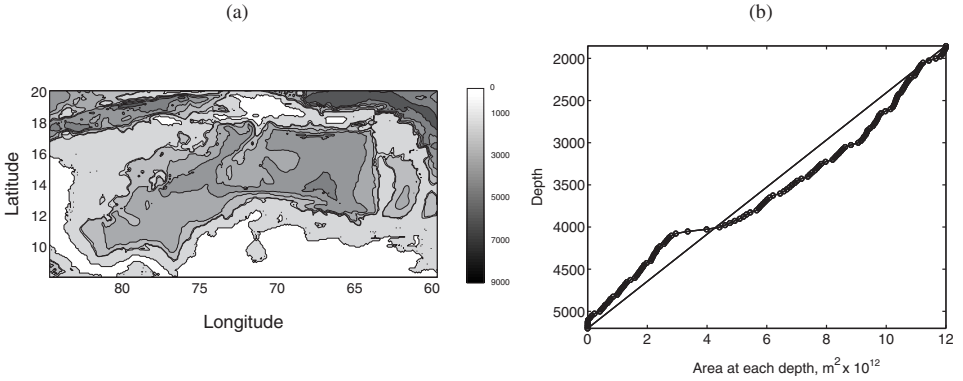

Figure 10. (a) Bathymetry of the deep Caribbean below 1850 m. A dense density current periodically flows through the Jungfern–Grappler sill complex, located near the Virgin Islands at 65° East, 17.6° North. (b) The cumulative depth histogram, showing that the bathymetry can be represented as a two-dimensional wedge. Data from MacCready *et al.* (1999).

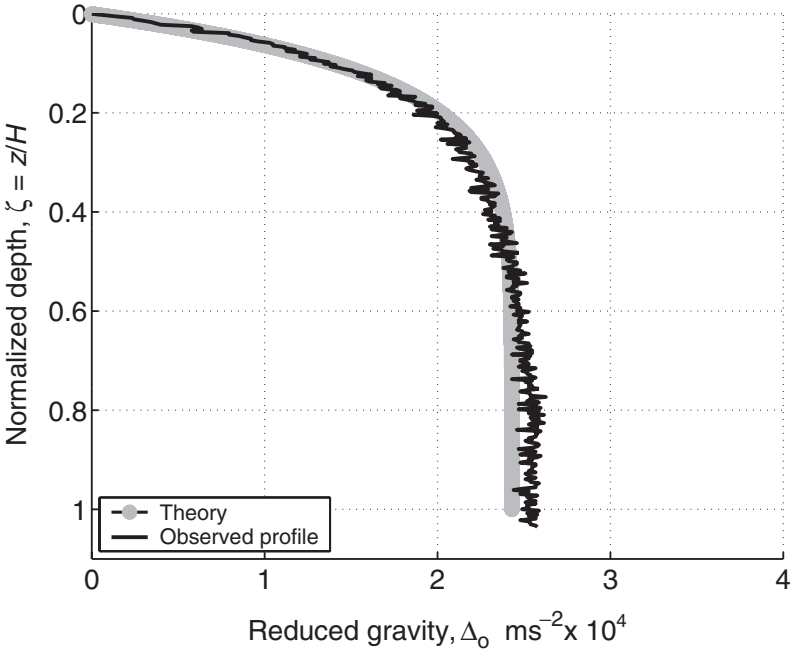

Figure 11. The density profile in deep Caribbean plotted against the theoretical prediction of (26). Field data from MacCready *et al.* (1999).

Solving the advection–diffusion equation (22) using (25) results in an analytic solution for the gradient of the reduced gravity,

$$\frac{\partial \Delta_o}{\partial \zeta} = \left.\frac{\partial \Delta_o}{\partial \zeta}\right|_{\zeta=0} \exp\left\{-\frac{U_o H}{\kappa}[\zeta - \log(1-\zeta)]\right\}, \tag{26}$$

which can be integrated numerically to obtain the density profile. We can determine the appropriate eddy diffusivity κ by considering the flux of density across the level at which the plumes feed into the basins (depth $z = 1850\,\mathrm{m}$). The only input of density is the flux of $Q = 1 \times 10^5\,\mathrm{m^3\,s^{-1}}$ of water with an average density anomaly $0.022\,\mathrm{kg\,m^{-3}}$. For a steady-state density profile, this flux must balance a downwards diffusive flux over the entire area A of the basin so that

$$Q\Delta_\mathrm{o} = \kappa A \frac{\partial \Delta_\mathrm{o}}{\partial z}, \tag{27}$$

thereby providing an expression for κ.

From the data of MacCready *et al.* (1999) the buoyancy gradient is $\partial\Delta_\mathrm{o}/\partial z = 4.5 \times 10^{-7}\,\mathrm{s^{-2}}$ and the area of the basin is $1.2 \times 10^{12}\,\mathrm{m^2}$ at $z = 1850\,\mathrm{m}$. This implies that at this level the diapycnal eddy diffusivity is $\kappa = 4.1 \times 10^{-5}\,\mathrm{m^2\,s^{-1}}$. This value is comparable with measured diffusivities in most mid-ocean sites away from topography (Gregg 1989, Ledwell *et al.* 1993, Toole *et al.* 1994). The maximum basin depth is 5369 m, so the effective depth of the basin below 1850 m depth is $H = 3519\,\mathrm{m}$. We will assume that the vertical velocity $U(\zeta)$ decreases to zero as $\zeta \to 0$ and has a magnitude of $U_\mathrm{o} \sim Q/A = 10^{-7}\,\mathrm{m\,s^{-1}}$ and hence the group $U_\mathrm{o}H/\kappa$ has a value between 6 and 8. In figure 11 we find that a slightly lower value of $U_\mathrm{o}H/\kappa = 3.1$ fits the observed data well; the shape of the curve is entirely determined by the vertical variation of the upwelling velocity $U(\zeta)$. A more accurate estimate of the value of U_o will require a detailed understanding of how the entrainment coefficient varies with the slope and Coriolis parameter for a time-dependent density current, which we are presently examining in our laboratory. Similar values of diffusivity of $\kappa = 1\text{–}6 \times 10^{-5}\,\mathrm{m^2\,s^{-1}}$ were inferred by MacCready *et al.* (1999), for a steady balance between downwards diffusion and upwelling driven by a composite plume model of the 13 observed overflow events. Using a similar balance between non-uniform upwelling and downwards diffusion of heat, the vertical stratification of the deep Red Sea was also explained in a similar way by Manins (1973), using values for the diffusivity of $\kappa = 1.4 \times 10^{-5}\,\mathrm{m^2\,s^{-1}}$.

5. Conclusions

In this article, we have experimentally confirmed the theoretical predictions of the vertical velocities and density profiles given by the two-dimensional filling box model of Baines and Turner (1969) for two-dimentional density currents on seven different slopes between 16 and 90°. In all cases the density profiles and vertical velocities in the interior of the tank show that the density currents are actively entraining and forcing a non-uniform upwelling. Using these results we have measured the horizontal entrainment ratio E_eq for density currents on a slope, and using equation (7) we have inferred the entrainment as a function of along-slope distance E. As the slope vanishes, the former asymptotes to $E_\mathrm{eq} \to 0.08 \pm 0.005$, while the latter has $E \to 0$. There is good quantitative agreement between the measurements of E with the previous measurements of Ellison and Turner (1959) as the flows are of comparable Reynolds numbers. The observation that E_eq asymptotes to 0.8, lends strong support to the idea of Hughes and Griffiths (2005) that for most oceanographic density currents on small slopes, where entrainment per unit along-slope distance is small, entrainment per unit depth

of fall will have significant effects and thus a confined basin can have filling box dynamics such as a non-uniform upwelling rate.

A specific oceanographic example where a non-uniform upwelling may be important is the Caribbean basin, in which deep waters are observed to be periodically renewed by dense overflows (MacCready *et al*. 1999). We show that the stratification in the deep Caribbean basin can be described by a balance between non-uniform upwelling and vertical diffusion (similar to Hughes and Griffiths 2005), and find good agreement between the theory and observations for reasonable choices of vertical upwelling velocities and eddy diffusivities.

Acknowledgements

We would like to thank two anonymous reviewers, Graham Hughes, Herbert Huppert, Ross Griffiths, Parker MacCready and Jim Price for useful comments and constructive criticism of drafts of this article. We acknowledge the support of the GFD Summer program at WHOI, where we received feedback on this work, and the support of Yale University.

References

Alavian, V., Behavior of density currents on an incline. *J. Hydraul. Eng*., 1986, **112**, 27–42.

Baines, W.D. and Turner, J.S., Turbulent buoyant convection from a source in a confined region. *J. Fluid. Mech*., 1969, **37**, 51–80.

Baringer, M.O. and Price, J.F., A review of the physical oceanography of the Mediterranean outflow. *Marine Geology*, 1999, **155**, 63–82.

Barnett, S., The dynamics of buoyant release in confined spaces. PhD thesis, Cambridge University, 1991.

Bush, J.W.M. and Woods, A.W., Vortex generation by line plumes in a rotating stratified fluid. *J. Fluid Mech*., 1999, **388**, 289–313.

Cenedese, C., Whitehead, J.A., Ascarelli, T.A. and Ohiwa, M., A dense current flowing down a sloping bottom in a rotating fluid. *J. Phys. Ocean*., 2004, **34**, 188–203.

Dallimore, C., Imberger, J. and Ishikawa, T., Entrainment and turbulence in a saline underflow in Lake Ogawara. *J. Hydraul. Eng*., 2001, **127**, 937–948.

Ellison, T.H. and Turner, J.S., Turbulent entrainment in stratified flows. *J. Fluid Mech*., 1959, **6**, 423–448.

Fer, I., Lemmin, U. and Thorpe, S.A., Cascading of water down the sloping sides of a deep lake in winter. *Geophys. Res. Letts*., 2001, **28**, 2093–2096.

Fer, I., Lemmin, U. and Thorpe, S.A., Winter cascading of cold water in Lake Geneva. *J. Geophys. Res. Oceans*, 2002a, **107**, Art. No. 3060.

Fer, I., Lemmin, U. and Thorpe, S.A., Contribution of entrainment and vertical plumes to the winter cascading of cold shelf waters in a deep lake. *Limn. Oceanorg*., 2002b, **47**, 576–580.

Gregg, M.C., Scaling turbulent dissipation in the thermocline. *J. Geophys. Res*., 1989, **94**, 9686–9698.

Hughes, G.O. and Griffiths, R.W., A simple convective model of the global overturning circulation, including effects of entrainment into sinking regions, *Ocean Modeling*, 2005 (In press).

Hughes, G.O., Griffiths, R.W. and Mullarney, J.C., A steady filling box solution with zero net buoyancy flux. *15th Australasian Fluid Mechanics Conference*, 2005.

Killworth, P.D. and Turner, J.S., Plumes with time-varying plumes buoyancy in a confined region. *Geophys. Astrophys. Fluid Dynam*., 1982, **20**, 265–291.

Ledwell, J.R., Watson, A.J. and Law, C.S., Evidence for slow mixing across the pycnocline from an open-ocean tracer-release experiment. *Nature*, 1993, **364**, 701–703.

Linden, P., The fluid mechanics of natural ventilation. *Annu. Rev. Fluid Mech*., 1999, **31**, 201–238.

MacCready, P., Johns, W.E., Rooth, C.G., Fratantoni, D.M. and Watlington, R.A., Overflow into the deep Caribbean: effects of plume variability. *J. Geophys. Res. Oceans*, 1999, **104**, 25913–25935.

Manins, P.C., A filling box model of the deep Red Sea. *Mem. Soc. R. Sci. Liege*., 1973, **6**, 153–166.

Manins, P.C., Turbulent buoyant convection from a source in a confined region. *J. Fluid. Mech*., 1979, **91**, 765–781.

Monismith, S.G., Imberger, J. and Morison, M.L., Convective motions in the sidearm of a small reservoir. *Limn. Oceanorg*., 1990, **35**, 1676–1702.
Morton, B.R., Taylor, G. and Turner, J.S., Turbulent gravitational convection from maintained and instantaneous sources. *Proc. R. Soc. Lon.* A, 1956, **234**, 1–32.
Munk, W.H., Abyssal Recipes. *Deep-Sea Res*., 1966, **13**, 707–730.
Pierce, D.W. and Rhines, P.B., Convective building of a pycnocline: laboratory experiments. *J. Phys. Ocean*., 1996, **26**, 176–190.
Price, J.F. and Baringer, M.O., Outflows and deep-water production by marginal seas. *Prog. Ocean*., 1994, **33**, 161–200.
Princevac, M., Fernando, H.J.S. and Whiteman, D.C., Turbulent entrainment into natural gravity driven flows. *J. Fluid Mech*., 2005 (in press).
Taylor, G.I., Dynamics of a mass of hot gas rising in air. *USAEC Report MDDC-919* (*LADC-276*), 1948, Los Alamos Scientific Laboratory, National Technical Information Service, Springfield, VA.
Toole, J.M., Polzin, K.L. and Schmitt, R.W., Estimates of diapycnal mixing in the abyssal ocean. *Science*, 1994, **264**, 1120–1123.
Turner, J.S., Turbulent entrainment – the developement of the entrainment assumption and its application to geophysical flows. *J. Fluid. Mech*., 1986, **173**, 431–471.
Turner, J.S., Stratification and circulation produced by heating and evaporation on a shelf. *J. Mar. Res*., 1998, **56**, 885–904.
Wells, M.G., Griffiths, R.W. and Turner, J.S., Competition between distributed and localized buoyancy fluxes in a confined volume. *J. Fluid. Mech*., 1999, **391**, 319–336.
Wells, M.G. and Sherman, B., Stratification produced by surface cooling in lakes with significant shallow regions. *Limn. Oceanorg*., 2001, **46**, 1747–1759.
Wong, A. and Griffiths, R.W., Stratification and convection produced by multiple turbulent plumes. *Dyn. Atmos. Oceans*., 1999, **30**, 101–123.
Wong, A., Griffiths, R.W. and Hughes, G.O., Shear layers driven by turbulent plumes. *J. Fluid. Mech*., 2001, **434**, 209–241.
Wright, S.J. and Wallace, R.B., Two-dimensional buoyant jets in a stratified fluid. *Proc. ASCE, J. Hydraul. Div*., 1979, **105**, 1393–1406.